ECCOMAS Congress 2016
VII European Congress on Computational Methods in Applied Sciences and Engineering
M. Papadrakakis, V. Papadopoulos, G. Stefanou, V. Plevris (eds.)
Crete Island, Greece, 5–10 June 2016

ACCELERATION OF MESH-BASED PHYSICAL OPTICS FOR ELECTROMAGNETIC SCATTERING ANALYSIS

Dao P. Xiang[1], and Matthys M. Botha[2]

[1]Department of Electrical and Electronic Engineering, Stellenbosch University
Private Bag X1, Matieland 7602, Stellenbosch, South Africa
e-mail: {17745349,mmbotha}@sun.ac.za

Keywords: Computational electromagnetics, Electromagnetic scattering, Physical optics (PO), Shadowing determination, Recursive update, Multilevel fast multipole method (MLFMM).

Abstract. *This work is concerned with scattering analysis of electrically large, conducting objects, using the physical optics (PO) approximation. Such analysis is important for radar cross section (RCS) calculations. Scattering objects are represented by a mesh of sub-wavelength sized triangle elements. Upon the mesh, the induced surface current density is represented by standard divergence-conforming basis functions. This is the mesh-based PO approach. It can be applied to take only a single reflection off the scatterer into account, as well as to take multiple, internal reflections into account. Both plane wave and point source illuminations are considered. The paper discusses computational challenges with regards to the fast and robust implementation of mesh-based PO analysis methods. These challenges are shadowing determination, in which the visibility of mesh elements with respect to source locations must be determined, as well as the fast evaluation of observed fields. A multi-level, buffer-based algorithm for efficient, single-reflection shadowing determination is outlined. It is also shown how the recursive field calculations required in the multiple-reflection PO, can be accelerated with the aid of the multilevel, fast multipole method (MLFMM), when the scattering object does not support any internal shadowing. Preliminary results illustrate the current status of this ongoing work on the acceleration of mesh-based PO analysis methods.*

1 INTRODUCTION

This work is concerned with scattering analysis of electrically large, conducting objects, using the physical optics (PO) approximation [1]. Such analysis is important for radar cross section (RCS) calculations. Scattering objects are represented by a mesh of sub-wavelength sized triangle elements. Upon the mesh, the induced surface current density is represented by standard divergence-conforming basis functions also used in the Method of Moments (MoM). This is the mesh-based PO approach [2, 3]. This approach can be applied to take only a single reflection off the scatterer into account (when illuminated by a plane wave or point source [Hertzian dipole]), as well as to take multiple, internal reflections into account. In the multiple-reflection case, the PO approximation is applied iteratively. In the interest of brevity, the paper will only be concerned with the standard RWG-type of mixed first-order, edge-associated basis functions, as employed in e.g. [2].

The paper starts off by briefly reviewing the above mesh-based PO analysis methods in Section 2. The computational challenges for the efficient (fast and robust) computer implementation of these methods are also discussed in Section 2. These include shadowing determination and the fast evaluation of observed fields. The main contribution of this paper follows in Sections 3, 4 and 5. Solutions are proposed to some of these challenges. Preliminary results are included, to illustrate the current status of this ongoing work on the acceleration of mesh-based PO analysis methods.

2 REVIEW OF MESH-BASED PHYSICAL OPTICS FOR PEC SCATTERERS

2.1 The PO approximation

Firstly, it is noted that for a magnetic field $\boldsymbol{H}^{\mathrm{inc}}$, incident upon an infinite perfect electrically conducting (PEC) half space, the exact solution of the induced surface current is

$$\boldsymbol{J}_s = 2\hat{n} \times \boldsymbol{H}^{\mathrm{inc}} \tag{1}$$

where $\hat{n}$ is the unit normal vector at the interface, pointing away from the PEC region. This simple result is the inspiration for the PO approximation [1, 4], which states that the surface current on a PEC object can be approximated in terms of the incident magnetic field and the outward-pointing unit vector to the surface, as follows:

$$\boldsymbol{J}_s = \begin{cases} 2\hat{n} \times \boldsymbol{H}^{\mathrm{inc}} & \text{for visible surfaces} \\ 0 & \text{for shadowed surfaces.} \end{cases} \tag{2}$$

The status of a location as being visible or in shadow, is established by determining whether there is line-of-sight visibility to the source, or not. For an incident plane wave as source, this means visibility towards infinity, along the negative of the incident direction. For a point source, visible status means an unobstructed view of the source point, from the given position on the scatterer surface.

2.2 The single-reflection PO method

The single-reflection PO method (SRPO) employs the PO approximation directly, to establish an approximate solution for the induced current density on a PEC scatterer. In order to achieve this, two tasks must be performed: (i) shadowed and visible parts of the scatterer must be identified; and (ii) in the visible regions, the known incident field must be mapped to a description of the surface current. The second of these tasks is quite straightforward in the mesh-based PO context: a local projection procedure is used to obtain the RWG basis function coefficient values, such that they best approximate the tangential components of the incident field according to (2) (see e.g. [2]). This is an $\mathcal{O}(N)$ task, where N denotes the number of mesh elements. The first task is much more challenging, with regards to computational efficiency.

2.3 The multiple-reflection PO method

The first step in the multiple-reflection PO method (MRPO) is to calculate the SRPO solution. This solution is denoted by $\boldsymbol{J}^{(0)}$. It is obtained in the illuminated regions of the scatterer's surface, according to the PO approximation and the local projection procedure:

$$\boldsymbol{J}^{(0)}(\boldsymbol{r}) = 2\hat{n} \times \boldsymbol{H}^i(\boldsymbol{r}). \tag{3}$$

In the case where multiple reflections are important, the cumulative radiation from parts of this current distribution is significant towards other parts of the object. Additional currents are induced according to the PO approximation, which represent a second reflection. In general, the current after l additional reflections is found by way of the following recursive expression [5]:

$$\boldsymbol{J}^{(l)}(\boldsymbol{r}) = \boldsymbol{J}^{(0)}(\boldsymbol{r}) + 2\hat{n} \times \fint_S \delta(\boldsymbol{r}')\boldsymbol{J}^{(l-1)}(\boldsymbol{r}') \times \hat{R}\frac{e^{-jkR}}{4\pi R}\left(jk + \frac{1}{R}\right) dS' \tag{4}$$

where $\boldsymbol{R} = \boldsymbol{r} - \boldsymbol{r}'$, $R = |\boldsymbol{R}|$, $\hat{R} = \boldsymbol{R}/R$; $\boldsymbol{r}'$ and $\boldsymbol{r}$ relate to the position vectors of the source and observation points, respectively, on the scatterer's surface. The scatterer's surface is denoted by S. The symbol $\fint$ represents the principle value integral. The factor $\delta(\boldsymbol{r}')$ is the shadowing coefficient, which takes on the value of either 1 or 0, depending on whether the current source point is visible to the observation point, or not.

In other words, the currents re-radiate iteratively, to excite a new set of PO currents at each reflection. The iteration process can be stopped after a pre-specified number of reflections based on the number of expected significant reflections supported by a given model, or until an adequately converged solution is obtained.

2.4 Computational challenges

For the mesh-based SRPO, the main challenge is to determine the shadowing status of each mesh edge, with respect to the illuminating source. A naïve approach would involve considering each edge in turn, and testing all elements for shadowing relative to the source. This would require $\mathcal{O}(N^2)$ operations ($\mathcal{O}(N)$ tests per edge, of which there are a total of $\mathcal{O}(N)$). Given that the other main task is projection, the cost of which is $\mathcal{O}(N)$, shadowing is clearly the bottleneck. This cost can be reduced by making use of the field-of-view buffer concept [6, 7, 3]. A buffer plane is defined upon an eikonal surface of the incident wave. This plane is subdivided into buffer boxes and each mesh element is listed in those boxes into which parts of it project. To test the shadowing status of a given point, it is also projected into the buffer to determine the box it falls into. Subsequently, only shadowing checks need to be performed against those elements which are listed for that particular buffer box. The present authors have been working on efficient shadowing algorithms which employ this general concept [8, 9]. The present status of this ongoing work is reviewed in Sections 3 and 4.

For the mesh-based MRPO, there are two main challenges. The first challenge is the calculation of subsequent incident fields due to the induced surface current, by way of (4). When using standard integration, the cost of this step is $\mathcal{O}(N^2)$, since at every mesh edge, the field must be calculated due to all other mesh elements. This step could be accelerated with a fast field calculation method. Indeed, this has been done using the fast far field approximation (FaFFA) [10, 11], which reduces the cost to $\mathcal{O}(N^{5/3})$. However, seeing that field calculation at a specified set of points can be viewed as a Method of Moments (MoM) type of matrix-vector product, the multilevel, fast multipole method (MLFMM) [12] could be used to reduce the cost of this step even further, to $\mathcal{O}(N \log N)$. Ongoing work in this direction, is reviewed in Sections 5.

The second challenge for the mesh-based MRPO, is efficient shadowing determination. The shadowing status of all mesh edges, as observed from every mesh edge projection point, is required. A naïve approach would require $\mathcal{O}(N^2)$ operations for every projection point (as explained above) and hence $\mathcal{O}(N^3)$ operations in total. Furthermore, the shadowing data would require $\mathcal{O}(N^2)$ storage space, except if calculated on-the-fly. To reduce this cost to a practically feasible scale, is a challenging task. There are however various problems of practical interest where all projection points are visible to all induced current sources. In such cases the shadowing information is trivial and acceleration of the field calculations do suffice. In this paper, the application focus of the MRPO is on such cases.

3 ACCELERATION OF SHADOWING DETERMINATION FOR THE SRPO WITH PLANE WAVE ILLUMINATION

3.1 Method

In this case, the eikonal surfaces are flat planes transverse to the direction of propagation of the incident wave. The buffer plane is chosen to be such a surface. The steps followed in the shadowing determination algorithm are as follows:

1. Triangles are projected into the buffer plane and the overall buffer bounding box is established, as well as bounding boxes for each projected element.

2. The objective of the algorithm is to separate triangles into small groups in the buffer plane, according to a buffer plane subdivision. Therefore, divide the plane into buffer boxes of which the size is proportional to the average mesh size. If a box is found which contains an excessive number of elements, then that box is again subdivided according to the same procedure. This yields a multi-level subdivision, capable of handling strongly inhomogeneous meshes as well. In case of a homogeneous mesh, only the first-level subdivision is typically necessary.

3. Now project each edge mid-point into the buffer and do shadowing testing against only those elements listed in the specific buffer box. This yield the visibility status of each corresponding, edge-associated basis function.

Above, some technical details of the algorithm are omitted in the interest of brevity. Also, the above description assumes that no grazing incidence is present. Grazing incidence occurs when the propagation direction of the incident plane wave is close to tangential to certain constituent surfaces of the scatterer. In such cases many elements may end up being listed in individual buffer boxes. The grazing triangles must then be handled with a custom procedure, similar to the one noted in [8].

3.2 Results

Figure 1 shows examples of the meshes used for shadowing evaluation testing. All meshes represent the same simple model, but will serve to illustrate the capabilities of the algorithm. The series of meshes are of a sphere which is inhomogeneously meshed and progressively refined, as explained in the figure. These progressively refined meshes are used to generate the shadowing determination runtime results shown in Figure 2, as a function of the number of mesh elements. On the same computational platform, results were also generated with the commercial mesh-based PO solver available as part of the FEKO software suite [13]. The direction of incidence is set to be aligned with the point around which the mesh is refined. The results show that the proposed, multilevel buffer subdivision scheme is significantly more efficient than the commercial solver. This is due the effective separation of mesh elements in the buffer, through appropriate localized subdivision. The observed time scaling for the proposed method is of $\mathcal{O}(N)$.

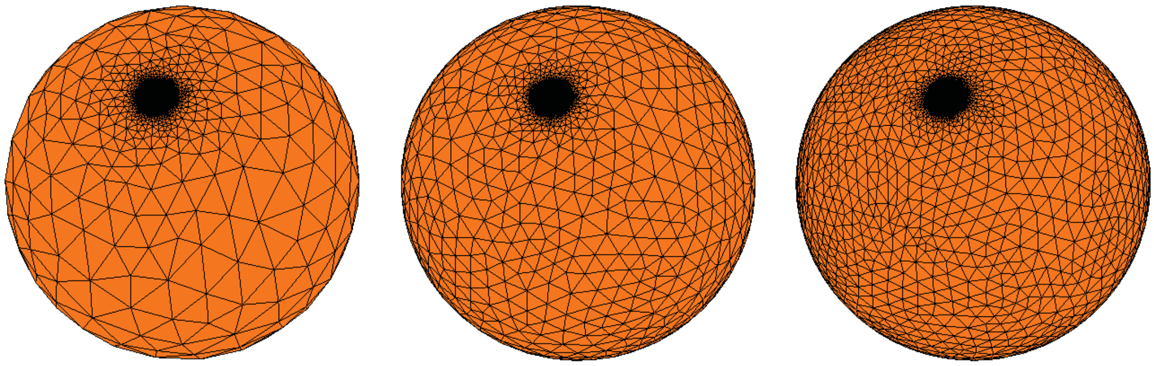

Figure 1: Progressively refined meshes of a conducting sphere. The sphere has a radius of $1\,\mathrm{m}$. The meshes are all inhomogeneous with a relative element size reduction factor of 100, around a single point.

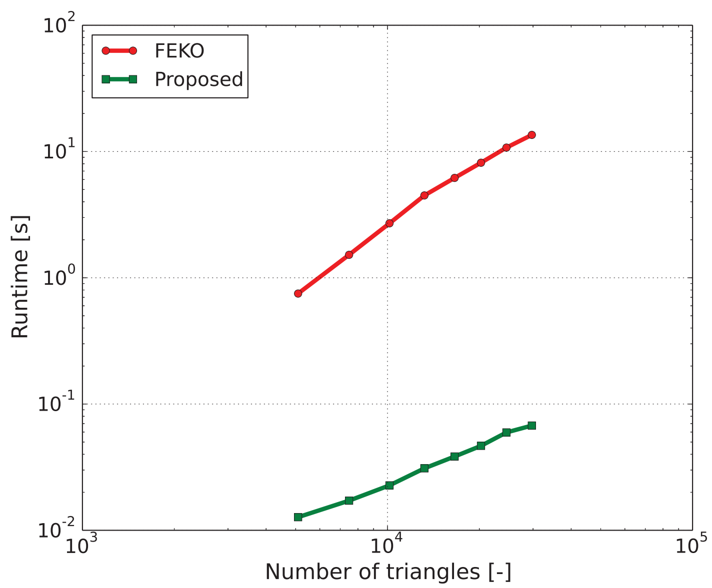

Figure 2: Shadowing determination runtime as a function of the number of mesh elements, for plane wave illumination of the inhomogeneous meshes shown in Figure 1. The proposed method is compared to a commercial solver.

4 ACCELERATION OF SHADOWING DETERMINATION FOR THE SRPO WITH POINT SOURCE ILLUMINATION

4.1 Method

In this case, the eikonal surfaces are spheres centred around the illuminating point source and the spherical coordinate system variables (θ, ϕ) are used to describe point locations in the buffer. Otherwise, the general procedure is the same as discussed above for the plane wave case. It is important to note that even in the case of a homogeneous mesh, the projected representation in the buffer plane is often inhomogeneous, due to the specific properties of the spherical coordinate system. This is a further important motivating factor for the recursive buffer subdivision approach. In the interest of brevity, a discussion on the case of grazing incidence for point source illumination will be deferred to a future publication.

4.2 Results

The set of progressively refined meshes described in Figure 1 is again used. The point source is placed normally above the point on the sphere around which the refinement is centred, at a height of $10^{-2}\,\mathrm{m}$. Figure 3 shows the shadowing determination runtime as a function of the number of mesh elements. Again, the results show that the proposed, multilevel buffer subdivision scheme is much more efficient than the commercial solver and that the cost scales as $\mathcal{O}(N)$.

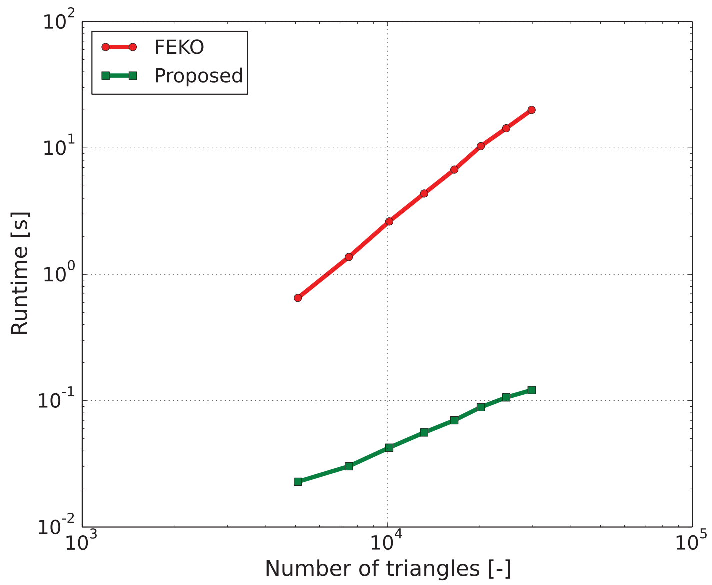

Figure 3: Shadowing determination runtime as a function of the number of mesh elements, for point source illumination of the inhomogeneous meshes shown in Figure 1. The proposed method is compared to a commercial solver.

5 MLFMM-BASED ACCELERATION OF INDUCED CURRENT CALCULATION IN THE MRPO

5.1 Method

To calculate the next solution according to the iterative MRPO expression (4), the observation point $\boldsymbol{r}$ must be placed at each edge mid-point in the mesh. Collectively, this can be expressed as a system of linear equations:

$$I^{(l)} = I^{(0)} + AI^{(l-1)} \tag{5}$$

where $I^{(l)}$ represents the vector of current coefficients after l additional reflections and $I^{(0)}$ represents the vector of current coefficients corresponding to the initial, single-reflection PO current. The dimension of square matrix A is $\mathcal{O}(N)$. The cost of conventionally evaluating the matrix-vector product $AI^{(l-1)}$ is thus $\mathcal{O}(N^2)$.

The matrix A in (5) can be split up into a sparse near-interaction matrix and the remaining far-interaction part, per the specifications of the MLFMM algorithm [12]:

$$I^{(l)} = I^{(0)} + \left(A^{\text{near}} + A^{\text{far}}\right) I^{(l-1)}. \tag{6}$$

The cost of the matrix-vector product $A^{\text{near}}I^{(l-1)}$ is $\mathcal{O}(N)$. Using the MLFMM, the matrix-vector product $A^{\text{far}}I^{(l-1)}$ has cost $\mathcal{O}(N \log N)$ (see e.g. [12] for further details). This can be compared with the scaling achieved using FaFFA acceleration, which as noted already, is given as $\mathcal{O}(N^{5/3})$ in [11].

5.2 Results

Consider the trihedral structure shown in Figure 4. It is illuminated by a plane wave with incident angles $\theta^{\text{inc}} = 45°$ and $\phi^{\text{inc}} = 45°$. It is homogeneously meshed with mesh size of $\lambda_0/10$, where λ_0 denotes the free space wavelength. On the illuminated side, all triangles are visible to each other, thus shadowing determination is trivial and consequently, the MRPO can be accelerated with the MLFMM in this case. Three reflections are incorporated with the MRPO ($l = 2$). Figure 5 shows how the runtime for the solution scales as a function of the number of mesh elements. Different data points are obtained by varying the excitation frequency (and thus wavelength) and remeshing (the frequency range used is $0.5\,\text{GHz}$ to $2.25\,\text{GHz}$). Clearly, the standard MRPO scales as $\mathcal{O}(N^2)$, due to the conventional evaluation of the matrix-vector product in (5). The MLFMM-accelerated MRPO has much lower runtime and as N becomes larger, the relative saving becomes increasingly significant. Note that $\mathcal{O}(N \log N)$ behaviour cannot be clearly observed in these preliminary accelerated results. This is ongoing work and further tests are still being conducted.

6 CONCLUSIONS

Computational challenges with regards to the fast implementation of mesh-based PO methods for scattering analysis of conducting objects, were discussed. Both single-reflection and multiple-reflection formulations were considered. These challenges are efficient shadowing determination and efficient calculation of observed fields. A multi-level, buffer-based algorithm for efficient, single-reflection shadowing determination was outlined and results were presented for a strongly inhomogeneous mesh. The results exhibit linear time scaling and are superior to the runtimes achieved with the commercial PO solver in FEKO. It was further shown how the recursive field calculations required in the MRPO, can be accelerated with the aid of the

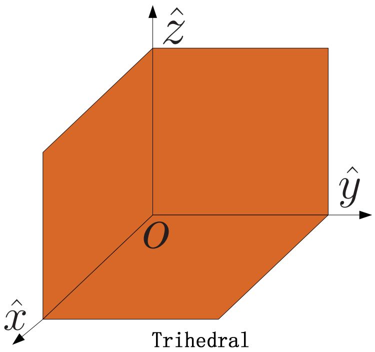

Figure 4: Conducting plate, trihedral model. The plate dimensions are all $1\,\mathrm{m}$.

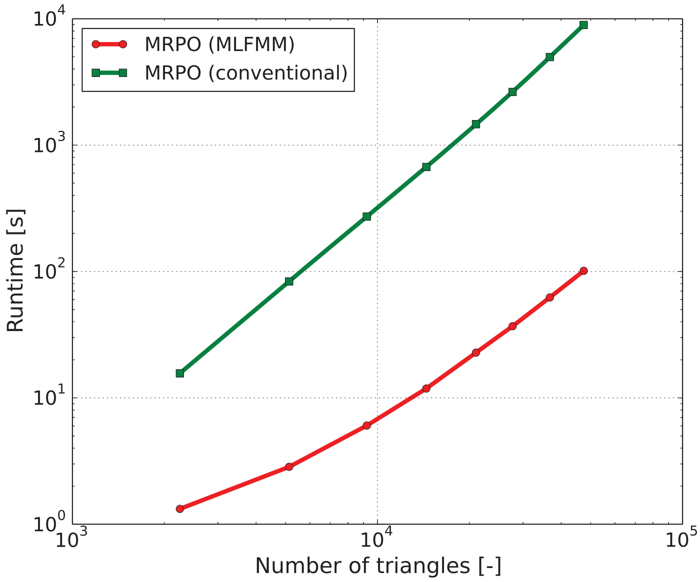

Figure 5: Runtime as a function of the number of mesh elements, for the conventional and MLFMM-accelerated MRPO implementations.

MLFMM. Preliminary results demonstrate significantly reduced runtime, when the scattering object does not support any internal shadowing.

ACKNOWLEDGMENT

This work was funded by Altair Development S.A. (Pty) Ltd, developers of the EM simulation software suite FEKO.

REFERENCES

[1] N. Bojarski, “A survey of the physical optics inverse scattering identity,” *IEEE Trans. Antennas Propag.*, vol. 30, no. 5, pp. 980–989, 1982.

[2] U. Jakobus and F. M. Landstorfer, “Improved PO-MM hybrid formulation for scattering

from three-dimensional perfectly conducting bodies of arbitrary shape," *IEEE Trans. Antennas Propagat.*, vol. 43, no. 2, pp. 162–169, 1995.

[3] F.-T. Zha, S.-X. Gong, Y.-X. Xu, Y. Guan, and W. Jiang, "Fast shadowing technique for electrically large targets using z-buffer," *Journal of Electromagnetic Waves and Applications*, vol. 23, no. 2-3, pp. 341–349, 2009.

[4] W. L. Stutzman and G. A. Thiele, *Antenna Theory and Design*. New York: John Wiley and Sons, 2nd ed., 1998.

[5] F. Obelleiro-Basteiro, J. Luis Rodriguez, and R. J. Burkholder, "An iterative physical optics approach for analyzing the electromagnetic scattering by large open-ended cavities," *IEEE Trans. Antennas Propag.*, vol. 43, no. 4, pp. 356–361, 1995.

[6] E. A. Haines and D. P. Greenberg, "The light buffer: A shadow-testing accelerator," *IEEE Computer Graphics and Applications*, pp. 6–16, September 1986.

[7] J. M. Rius, M. Ferrando, and L. Jofre, "GRECO: Graphical electromagnetic computing for RCS prediction in real time," *IEEE Antennas and Propagation Magazine*, vol. 35, no. 2, pp. 7–17, 1993.

[8] D. P. Xiang and M. M. Botha, "Aspects of efficient shadowing calculation for physical optics analysis of meshed objects," in *Proceedings of the International Conference on Electromagnetics in Advanced Applications (ICEAA '14)*, pp. 492–495, Aug 2014. Aruba, Dutch Antilles.

[9] D. P. Xiang and M. M. Botha, "Further progress with fast and reliable shadowing determination for mesh-based po analysis," in *Proceedings of the International Conference on Electromagnetics in Advanced Applications (ICEAA '15)*, pp. 958–961, Sept 2015. Torino, Italy.

[10] C.-C. Lu and W. C. Chew, "Fast far-field approximation for calculating the RCS of large objects," *Micro. Opt. Tech. Lett.*, vol. 8, no. 5, pp. 238–241, 1995.

[11] R. J. Burkholder, "A fast and rapidly convergent iterative physical optics algorithm for computing the RCS of open-ended cavities," *Applied Computational Electromagnetics Society Journal*, vol. 16, no. 1, pp. 53–60, 2001.

[12] W. C. Chew, E. Michielssen, J. Song, and J. Jin, *Fast and efficient algorithms in computational electromagnetics*. Artech House, Inc., 2001.

[13] Altair Engineering Inc, "FEKO User's Manual Suite 7.0," August 2014. http://www.feko.info.